Chapter 1

CONTROLLING FLUID PROPERTIES THROUGH POLYMER ADDITIVES

This chapter covers applications of polymers as rheological modifiers (Section 1.1), essential ideas in polymer physics and rheology leveraged in the contained work (Section 1.2), a description of the theory and practice of dripping-onto-substrate extensional rheometry (Section 1.3), and a brief introduction to megasupramolecules (Section 1.4). This chapter is intended as a broad overview to introduce a more general audience to the core ideas in the thesis and is by no means exhaustive.

1.1 Desirable Effects of Polymer Additives on Solution Properties

Polymer additives are a ubiquitous part of the industrial toolkit for modifying the rheology (and other properties) of fluids in transportation, manufacturing, and consumer use. In this section, I will discuss three key applications where high extensional resistance is desirable and where there is an unmet need due to the vulnerability of existing additives to mechanical degradation.

Mist Control

When a liquid is sprayed, the average drop size and distribution of drop sizes determine much of the resulting behavior.[1,2] In agricultural spraying applications, small droplets may drift, while large droplets may rebound off leaves (as discussed more below).[2–8] In a fuel injector in an engine, drops must be small and uniform enough to rapidly and completely combust.[9] In an accidental release of a flammable fluid, small droplets can quickly evaporate and contribute to a fire in the presence of an ignition source.[10–12]

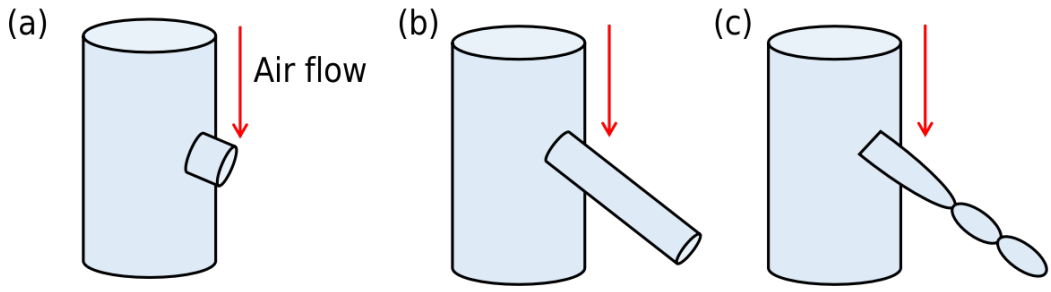

Figure 1.1: Ligament formation and pinchoff. (a) An instability results in a protrusion of the fluid into the surrounding stream. (b) A ligament forms and extends from the main body of the fluid. (c) The ligament pinches off under the capillary action of surface tension.

Controlling both the drop size and the distribution is thus desirable. Polymeric additives are attractive for many mist control and antimisting applications because they have a profound effect on the breakup of jets into drops without greatly increasing the shear viscosity (see Section 1.2 below for discussion of modification of shear versus extension). When a polymer is added into a fluid that is then sprayed, the fluid is observed to form drops of larger average size[2,10,11,13] and fewer tiny satellite droplets.[3,14]

The effect on jet and spray breakup by polymers can be attributed to their resistance to elongational flow. When a jet is breaking up, instabilities cause perturbations extending into the surrounding flow (Figure 1.1(a)). As the surrounding flow extends these perturbations, thin ligaments of fluid are formed (Figure 1.1(b)) and extend. As the ligaments extend, surface tension is driving pinchoff into droplets (Figure 1.1(c)). This process is highly extensional, and a polymer solution will strongly resist that pinchoff, leading to suppression of droplet formation and larger droplets if pinchoff still occurs.[14,15]

Droplet Deposition

When a fluid droplet impacts a surface, it experiences one of multiple fates. It could rebound and leave the surface, it could slide along an angled surface and

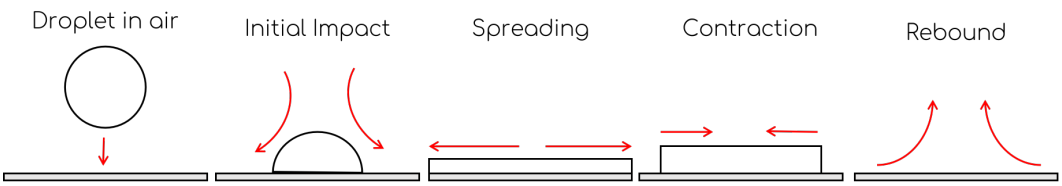

Figure 1.2: Typical stages of droplet impact and rebound. Left-to-right: pre-impact, impact, spreading, contraction, and rebound.

fall off, or it could deposit and be retained. Understanding droplet deposition is important to a number of applications, from distributing fertilizers and pesticides to crops,[3,7,16] to applying coatings and paints to materials,[17,18] to uncovering how viral droplets stick to surfaces.[19]

When a droplet impacts a surface, the kinetic energy from falling results in a series of stages where the droplet impacts, spreads, contracts, and can then rebound (Figure 1.2). During spreading, the kinetic energy is translated into surface energy, which then drives the contraction and extent of rebound, depending on how much energy was dissipated due to viscosity and interaction with the surface.

When a high molecular weight polymer is added into the solution at very low treat rates (less than 0.1 wt %), the contraction is substantially slowed and rebound can be suppressed.[5,20] This effect occurs for multiple polymer backbones, indicating it is a physical interaction, rather than a chemical interaction with the surface.[5,21]

The initial hypothesis put forth to explain these dramatic changes in droplet behavior was that the polymer additives changed the bulk extensional viscosity and thus dissipated more energy, keeping surface tension from driving rebound as it does in the Newtonian case.[5,20] That conclusion, however, has been heavily contested in the literature with additional experiments and analysis. Follow-up experiments with small targets[15,22] and Leidenfrost drops (where

a thin layer of vapor is created between the drop and the surface)[23,24] show that the effect of the polymer additive disappears when surface interaction is removed, contracting that the modification to the bulk elongational properties is the source. Studies of the behavior at the contact line between the drop and the surface showed that the effect of the polymer appears to be concentrated at the contact line, where chains are strongly stretched.[21,25] While the bulk extensional properties appear to not be the direct cause, the extensional behavior (i.e., stretching) of the polymers in solution appears to be intimately tied to their ability to increase droplet retention on surfaces.[7]

Drag Reduction

When fluid is flowing, it experiences friction (drag) that must be overcome to continue flow. In transporting fluids long distances or circulating within a closed system, we use pumps to keep the fluid flowing, at great energy cost. A phenomenon discovered in the 1940s, polymeric drag reduction, reduces the drag experienced by a fluid during turbulent flow.[26–29] Increasing bulk Reynolds number ($Re = \rho UD/\eta_{shear}$, where ρ is the density, U is the mean velocity, D is the length scale of the flow, and η_{shear} is the shear viscosity) and increasing polymer concentration experimentally results in increased drag reduction, up to a maximum drag asymptote.[30,31]

Describing the mechanism driving polymeric drag reduction is an active field of study, due the complexity of both the polymer conformation behavior and the chaotic nature of turbulence.[32,33] When characterizing wall-bounded turbulent flow (such as that in a pipe), researchers identify eddies, coherent flow structures with an associated size and characteristic velocity that vary in time and space throughout the flow. Energy is transferred in the flow from the large scale eddies (on the order of the size of the geometry) to the smallest scale

where viscous dissipation dominates (the Kolmogorov scale).[34] To give a sense of the scale, at $Re = 50,000$, this smallest scale is $3 * 10^{-}4$ of the largest scale. Turbulence consists of a cycle of bursts and sweeps–high velocity eddies move towards the wall and interact with the slower flow near the wall (sweeps), causing that near-wall fluid to rapidly move away from the wall (bursts).[35] These bursts are highly elongational, which motivates characterizing the extensional properties of the dilute polymer solutions used in polymeric drag reduction.

The complexity of the field of drag reduction is discussed in more depth in Chapter 3.

Chain Scission

Long, covalently-bonded polymers are used as rheological modifiers in a vast number of applications, from paints to foods to construction. The specific applications just discussed—mist control, droplet deposition, and drag reduction—share a trait in common where these existing additives may not be useful: prior to their use, the fluid will often be pumped, mixed or otherwise subjected to a strong flow. Traditional polymer additives are highly prone to shear as their molecular weight increases. The study of chain scission has been of particular interest in the drag reduction community because it greatly limits where drag-reducing additives can be used industrially.[33,36–43]

Chain scission occurs at lower extension rates as molecular weight increases, although literature disagrees on the exact dependence.[44–49] Careful development of flow geometries were required to extract meaningful information about polymer behavior, and mischaracterization of the flow (i.e., laminar versus turbulent) in a number of studies has led to inconsistent relationships between extension rate and molecular weight of chain scission.[49] Chain scission studies primarily have used molecular weight distributions to characterize the inter-

action between flows and polymer additives, leading to relationships that are backbone dependent, rather than capturing underlying explanations from rheology or polymer physics. This specificity limits applicability to novel polymer additives, motivating further study.

1.2 Essential Polymer Physics and Rheology

Polymer Solution Regimes

A flexible polymer chain at equilibrium in solution adopts a coiled configuration, determined by the interaction between the solvent and the chain, and as concentration increases, the chain and the chains around it. These coils take up space in the solution, the "pervaded volume," and different regimes of polymer solution behavior occur depending on how much of the solution is pervaded by polymer (Figure 1.3). In the dilute regime, polymer coils do not interact, and each chain can be treated individually. As concentration increases, the polymer coils pervade more of the volume until they touch, a point we call the overlap concentration (c^*). Above the overlap concentration, the polymer chains begin to interact, changing the solution properties substantially—the semi-dilute regime. If the chains are long enough and the concentration is above the entanglement concentration, the chains will intertwine and create physical cross-links. In this work, we will focus primarily on concentrations at or below the overlap concentration for polymer backbones. Chapter 5 discusses some semi-dilute solutions.

The above narrative description of the overlap concentration hides nuance about what is the precise choice of when overlap occurs and that the transition between regimes is not necessarily sharp. The literature contains a number of answers, basing the definition on different measures of the size of the polymer coil. Throughout this work, Equation 1.1[50] (where $[\eta]$ is the intrinsic viscosity,

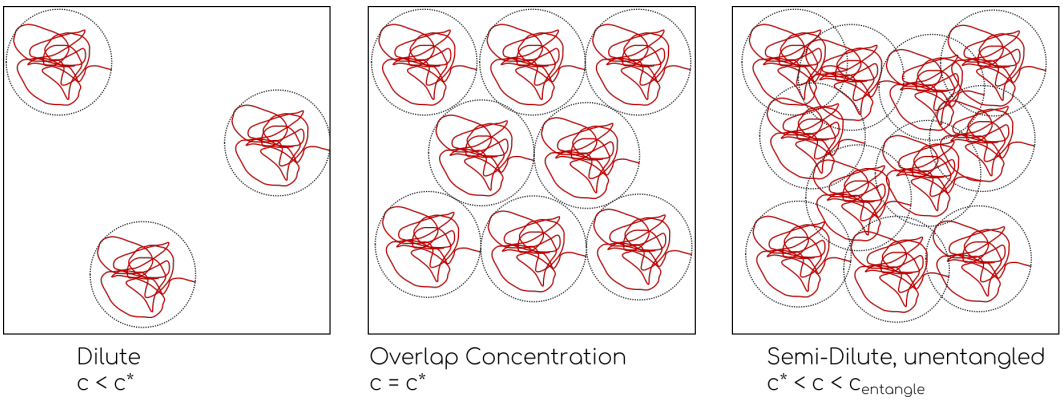

Figure 1.3: Regimes of low-to-moderate concentration (c) for polymer in solution. Left-to-right: Dilute solution (concentrations below overlap, $c < c^*$), overlap concentration (c^*), and semi-dilute, unentangled ($c^* < c < c_{entangle}$, where $c_{entangle}$ is the entanglement concentration).

discussed more below) will be used as the definition of overlap concentration, in order to facilitate comparisons to literature studies of dripping-onto-substrate extensional rheometry in which the same definition was applied. This definition is based on an average chain spacing of twice the radius of gyration at infinite dilution.

$$c^* = \frac{0.77}{[\eta]} \tag{1.1}$$

The overlap concentration is a function of both the polymer molecular weight and the interaction between the solvent and the backbone, as discussed below.

Solvent Quality

The size of a flexible polymer coil in dilute solution depends on the relative solvent-chain and chain-chain interaction. If the chain has no preference between intra-chain and solvent interactions, it will adopt an ideal random walk of its segments (accounting for steric hinderance and limited flexibility due to chemical bonds)—the fluid is a theta solvent. If the chain prefers the solvent to intra-chain interactions, the chain will swell—the fluid is a good solvent. If

the chain prefers intra-chain to solvent interactions, the coil will collapse and if concentration is sufficiently high, the polymer can precipitate. The overlap concentration, discussed above, captures the pervaded volume of a particular chain, and can be calculated from the intrinsic viscosity ($[\eta]$), a measure of the contribution of polymer to the shear viscosity at infinite dilution. The Kuhn-Mark-Houwink-Sakurada equation (Equation 1.2) is an empirical relationship between $[\eta]$ and molecular weight (M) for a particular polymer backbone-solvent-temperature combination.

$$[\eta] = K(M)^a \tag{1.2}$$

K is an empirical prefactor with units of $[\eta]$. In the studies in this work, K and $[\eta]$ will have units of 1/wt %, and the molecular weight M will be chosen to be the weight-average molecular weight M_w[51] with units of g/mol. The exponent a is often used as a proxy for solvent quality as a a value of 0.5 indicates the polymer-solvent combination is at the theta condition, where the chains are in their ideal configuration, and a greater than 0.5 indicates a swollen chain. For flexible chains, a reaches a maximum of 0.8 in a good solvent. a greater than 0.8 indicates a semi-flexible or rigid chain.

To compare a to other measures of solvent quality, Zimm theory scaling gives $[\eta] \sim M_w^{3\nu-1}$, where ν is the Flory exponent, i.e., the exponent relating the radius of gyration to the molecular weight. Thus, a can be related to the Flory exponent as $a \approx 3\nu - 1$. $\nu = 0.5$ indicates a theta solvent (ideal chain behavior) and $\nu = 0.6$ is the limit for a flexible chain in a good solvent.

Dilute Polymer Solutions in Shear Versus Extension

Every flow can be broken down into two components: shear and extension (Figure 1.4). A typical way to apply shear is by placing a material between two surfaces and moving one relative to the other. In shear, the stress is

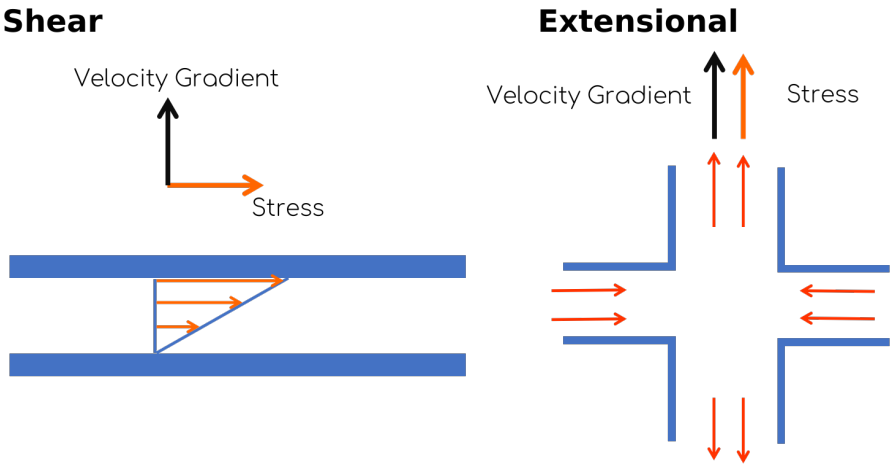

Figure 1.4: Diagram of shear versus extensional flow.

perpendicular to the velocity gradient. Extensional flows involve stretching fluid elements, such as in cross-slot flow or rapidly separating two plates with a material in between. In extension, stress is parallel to the velocity gradient.

The behaviors of dilute polymer solutions in shear and in extension differ strongly, particularly as the molecular weight of the polymer increases. In shear, polymer coils do not fully extend, and instead tumble with the flow. Addition of polymer in the dilute regime does increase the shear viscosity, but in very dilute solutions, that effect can be neglible. In extension, on the other hand, the effects of polymer addtives can be quite dramatic, with potential increases in the extensional viscosity of the solution of over 10,000. These large changes in the extensional properties are due to the polymer chains resisting the stretching of fluid elements. Additionally, the effects of concentration differ between shear and extension. Solutions that are considered dilute (below overlap concentration) in shear may exhibit inter-chain interactions in extensional flow, leading to stronger dependence on concentration for extensional properties.[52]

The ability to modify the extensional properties is dependent on the polymer backbone stiffness and extensibility, with flexible backbones having more impact on the flow.[53,54]

1.3 Dripping-onto-Substrate Extensional Rheometry (DoSER)

Because of the vast differences in polymer solution behavior in shear versus extension and the effects of these behaviors on mist control and drag reduction, measurements of these solutions in elongational flow fields can illuminate application-relevant properties. While polymer melt extensional rheology has long been part of the rheologist's toolbox, polymer solutions have presented additional challenges due to difficulties setting up an appropriate and controlled flow field, as clamping the ends of a sample is not feasible, and due to the increasingly low relaxation times as viscosity of the solution decreases, requiring higher speed flow field setup and measurement.[55–57] Capillary-breakup extensional rheometry (CaBER) solved many of these challenges for solutions with shear viscosities greater than 20 mPa-s by constructing a flow field by rapidly separating plates at a known rate and then observing the thinning of the midpoint of the formed liquid bridge using a laser micrometer.[55]

The minimum diameter of the liquid bridge (D) as a function of time (t) in capillary-breakup rheometry is observed to take on the characteristics of three regimes, depending on the relative properties of the fluid. In Newtonian fluids, two regimes are observed, controlled by the Ohnesorge number, $Oh = \eta_{shear}/\sqrt{\rho\sigma d}$ a dimensionless group comparing the viscous forces to the inertio-capillary forces, where η_{shear} is the shear viscosity of the fluid, ρ is the density of the fluid, σ is the surface tension, and d is a characteristic length scale.

In Newtonian fluids of high viscosity compared to inertia ($Oh > 1$), the liquid bridge thins according to Equation 1.3, a balance between viscous and capillary

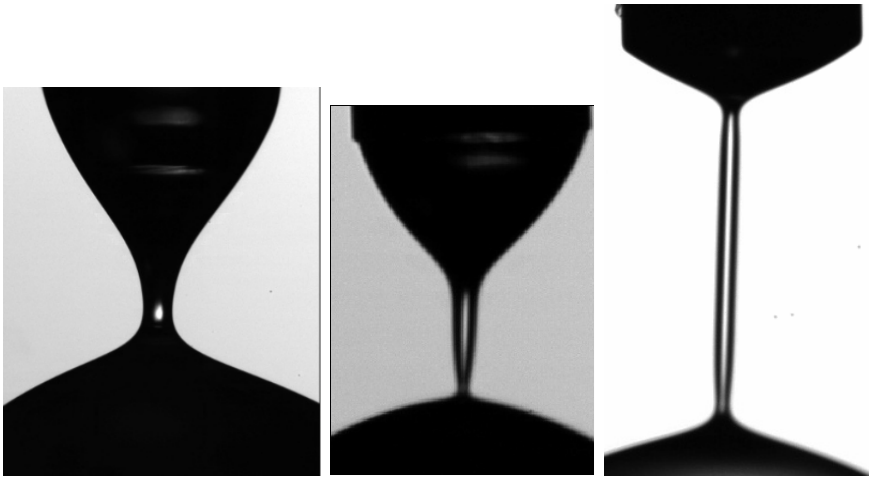

(a) Visco-capillary (polyalphaolefin). (b) Inertio-capillary (water). (c) Elastocapillary (6M PEO in water at 0.02 wt %).

Figure 1.5: Images demonstrating expected shapes of liquid bridge necks for the three regimes of capillary breakup.

(surface tension) forces, the visco-capillary regime.

$$\frac{D(t)}{D_0} = 0.0709\frac{2\sigma}{\eta_{shear}D_0}(t_p - t) \tag{1.3}$$

D_0 is the starting diameter of the liquid bridge. t_p is the pinchoff time. The neck of the liquid bridge forms a characteristic cylindrical shape in this regime (Figure 1.5a).[58]

In low viscosity Newtonian fluids, where $Oh \ll 1$, the inertial forces balance capillary forces in the inertio-capillary regime of thinning, following Equation 1.4.

$$\frac{D(t)}{D_0} = 0.8\left(\frac{t_p - t}{(\rho D_0^3/8\sigma)^{1/2}}\right)^{2/3} \tag{1.4}$$

The neck of the liquid bridge forms a characteristic conical shape in this regime (Figure 1.5b).[58]

In viscoelastic fluids, such as polymer solutions, the thinning is initially visco-capillary or inertio-capillary, depending on the value of Oh; however, if the elastic forces exceed the viscous or inertial forces respectively, the behavior

will transition to the elastocapillary regime where the balance of elastic and capillary forces controls the thinning (Figure 1.6). In capillary-breakup experiments, this transition occurs at a Weissenburg number ($Wi = \lambda_E \dot{\epsilon}$) of 2/3, where λ_E is the extensional relaxation time and $\dot{\epsilon}$ is the extensional strain rate. The liquid bridge observed in the elastocapillary regime is a cylinder (Figure 1.5c) that thins with a characteristic time scale related to the extensional relaxation time (Equation 1.5).

$$\frac{D(t)}{D_0} = \sum_i \left(\frac{g_i D_0}{4\sigma}\right)^{1/3} e^{-t/3\lambda_{E,i}} \approx \left(\frac{G D_0}{4\sigma}\right)^{1/3} e^{-t/3\lambda_E} \tag{1.5}$$

g_i and $\lambda_{E,i}$ are the corresponding extensional modulus and relaxation time for a mode i; throughout this work, we adopt the hypothesis of Entov and Hinch and assume that the longest relaxation time dominates the observed capillary-breakup behavior, and thus we can approximate the elastocapillary regime with a single modulus G and relaxation time λ_E.[58,59]

Because polymers are not ideal springs with the ability to extend infinitely, finite extensibility limits the duration of the elastocapillary regime, leading to a more rapid fall-off in the observed diameter at long time than expected from Equation 1.5 (Figure 1.6).

As solution viscosity decreases, either by using lower viscosity solvents or lowering polymer concentration, the duration of inertial effects due to the initial separation of the plates begins to exceed the liquid break-up time and thus the elastocapillary regime is not measurable. To solve this limitation with CaBER instruments, the Sharma group developed dripping-onto-substrate extensional rheometry (DoSER), a form of capillary-breakup extensional rheometry. In DoSER, a drop of fluid is dispensed from a nozzle (often a blunt-tipped needle) onto a substrate, and a liquid bridge forms between the nozzle and the substrate. The thinning of the liquid bridge is observed as a function of time

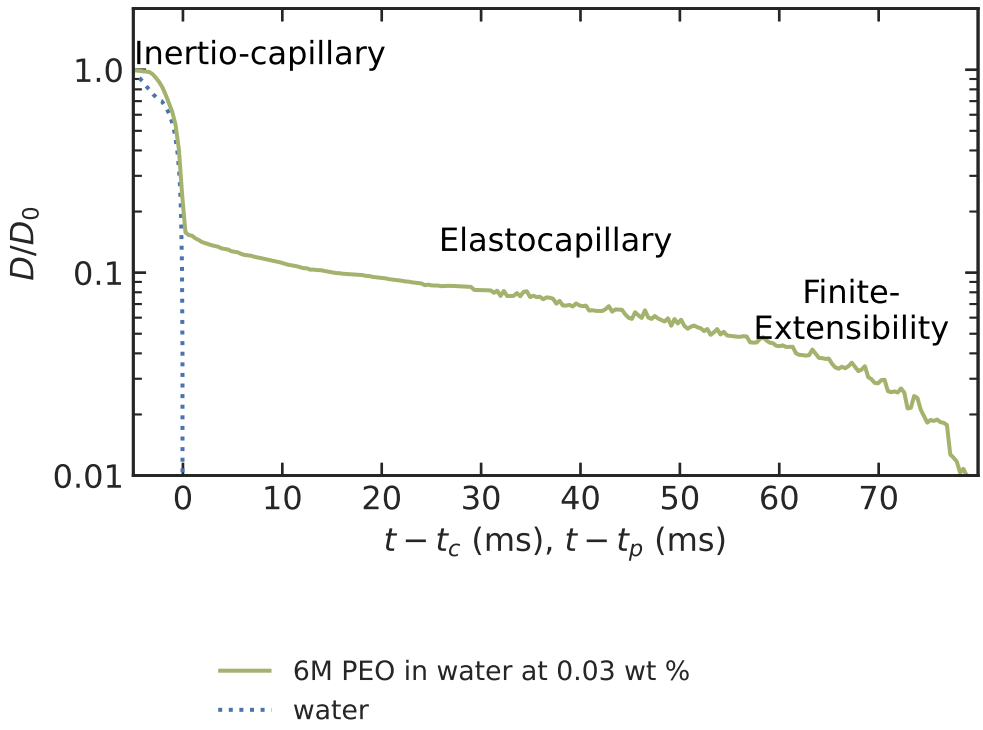

Figure 1.6: Example of measured capillary thinning for a polymer solution compared to water, demonstrating transitions for the polymer solution from the inertio-capillary regime (corresponding to water alone) to the elastocapillary regime, followed by finite-extensibility.

using a high-speed camera. Because the strain rate of thinning is imposed by the fluid rather than the separation of plates as in traditional CaBER, much higher strain rates are possible, allowing access to measurement of much smaller relaxation times, and correspondingly, lower solution viscosities. The lower limit on measurable relaxation times is controlled by the camera's spatial and temporal resolutions—small relaxation times require both high speeds and high resolution–as well as vibrations due to air currents and inertial ringing of the drop contacting the substrate obscuring the short time behavior. The upper limit on measureable relaxation times is primarily controlled by the memory available in the camera, which can be mitigated by recording at lower frame rates for high relaxation time samples.

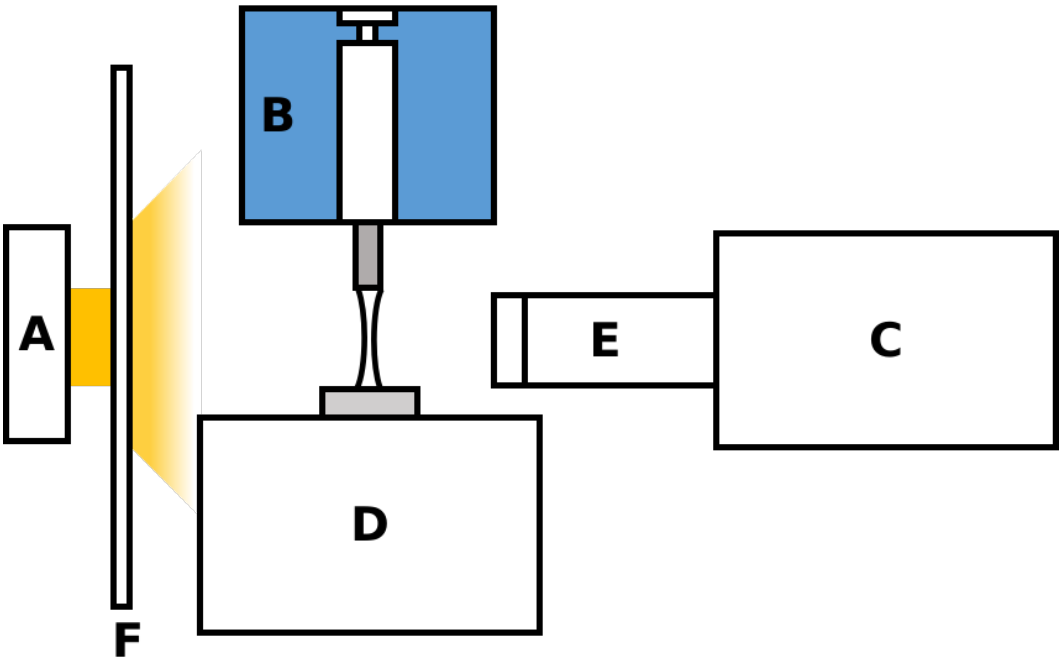

Figure 1.7: Schematic of dripping-onto-substrate extensional rheometer (not to scale).

DoSER Methodology

A dripping-onto-substrate extensional rheometry (DoSER) instrument (Figure 1.7) consists of a light source (**A**), a syringe pump for solution delivery (**B**), a (preferably high-speed) camera (**C**), an optical train that resolves the length scales desired (**E**), and a substrate (**D**). The light passes through a diffuser (**F**) before reaching the measurement plane. To set up the flow fluid, a syringe with a blunt-tip metal needle is attached to the syringe pump above the substrate holder.

The following is a brief discussion of our methodology for collecting and analyzing data using DoSER, further discussion of the analysis package we developed, dosertools, appears in Appendix A.

The substrate is chosen to be phobic to the solvent of the solution, such that a drop beads up, to prevent undesired additional flow fields away from the

primary extensional flow. The height between the substrate and nozzle is chosen based on the optimal range of height-to-initial-droplet-diameter—initial droplet diameter is a function of both nozzle diameter and surface tension of the solution.[60] Detailed discussion of selection of the height between the nozzle and the substrate is planned to be discussed in Robert Learsch's thesis.

DoSER experiments are performed using the following procedure. An aliquot is slowly loaded into a syringe through a blunt-tip needle. The syringe is attached to the syringe pump and the syringe pump is slowly advanced until solution is observed to drip from the needle. A clean set of aluminum substrates is loaded onto the substrate holder and the first substrate is aligned below the needle tip. The light is turned on and the camera is focused and aligned with the needle tip. The substrate is then raised or lowered to the correct height (as describe above) relative to the needle tip. A background video with a droplet-free needle and substrate is acquired. A drop is dispensed from the needle tip by the syringe pump at a rate of 0.02 mL/min, until the drop is nearly touching the substrate. The syringe pump is stopped prior to droplet-substrate contact. The droplet contact through liquid bridge formation and pinchoff is recorded (referred to as an experimental video or "run"). A new substrate is then placed below the needle tip. Dispensing drops onto a clean substrate is repeated until sufficient runs are recorded.

The data collected is processed using the *dosertools* Python package, developed by Robert Learsch and Red Lhota (Appendix A). A summary of the steps involved appears below.

The experimental and background videos are cropped to remove the substrate from the frame. The background is averaged and subtracted from the experimental video to remove any non-uniformity in pixel intensity due to the light

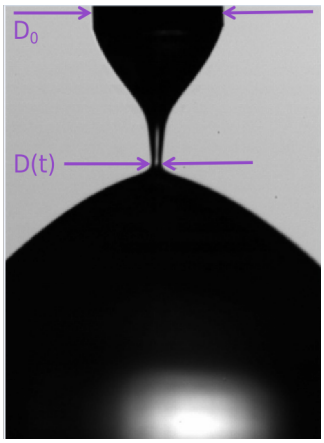

Figure 1.8: Example DoSER image showing the needle diameter D_0 and the minimum diameter of the liquid bridge $D(t)$.

source or lens. The resulting image is then turned into a binary image using an Otsu threshold. The minimum thread diameter is detected as a function of time, and normalized using the nozzle diameter (treated as the initial liquid bridge diameter, D_0, for thinning) (Figure 1.8). The needle diameter is measured from the experimental or background video, whichever video has the most clearly defined boundaries of the nozzle tip.

The normalized diameter is then analyzed to determine the critical time and the relaxation time. The critical time (t_c) is defined as the time of transition from the visco-capillary or inertio-capillary regime to the elastocapillary regime. Plotting normalized diameter data as a function of time past the critical time ($t - t_c$) removes differences between datasets due to when recordings were started relative to the physical behavior. Equation 1.5 can be rewritten as a function of $t - tc$ (Equation 1.6).

$$\frac{D(t)}{D_0} = \left(\frac{D_{tc}}{D_0}\right)^{1/3} e^{-(t-t_c)/3\lambda_E} \tag{1.6}$$

D_{tc} is the diameter at the critical time.

Prior literature determined the critical time by inspection.[53,54,57,58,61] Robert Learsch developed a method for detecting the critical time through finding the

moment of maximum strain rate within the window of normalized diameter in which transition occurs, which was implemented in the dosertools package. By finding the critical time systematically rather than by inspection, we significantly reduced user-to-user variation in analysis.

After finding the normalized diameter as a function of time past the critical time, Equation 1.6 is fit to the elastocapillary regime, chosen to have an upper bound of $D/D_0 = 0.1$ or D_{t_c}/D_0, whichever is lower, and a lower bound of 0.045. From this fit, the extensional relaxation time is calculated for each sample (fitting details in Appendix A).

1.4 Megasupramolecules

End-associative telechelic polymers of sufficiently long backbone length can associate in solution to form supramolecular polymer exceeding 1Mg/mol in total weight, called megasupramolecules (Figure 1.9). Each telechelic polymer unit acts as a unimer in this large polymer, and can reversibly associate and disassociate both at equilibrium and in flow. This reversibility gives long, end-associative telechelic polymers a substantial advantage over traditional, long-chain polymer additives because the ability to disassociate under strong flows can prevent chain scission.[12] The megasupramolecules exhibit an equilibrium distribution of linear and ring supramolecules—linear supramolecules have a larger rheological impact and thus are usually more desirable. By using pairwise association and keeping unimer lengths sufficiently long, the distribution can be biased towards linear megasupramolecules.[12,62]

Megasupramolecular systems have a number of aspects that can be tuned to achieve their desired rheological behaviors and thus their performance. The unimer backbone length can be adjusted depending on desired effective molecular weight after association, as long as it is neither too long (and thus vul-

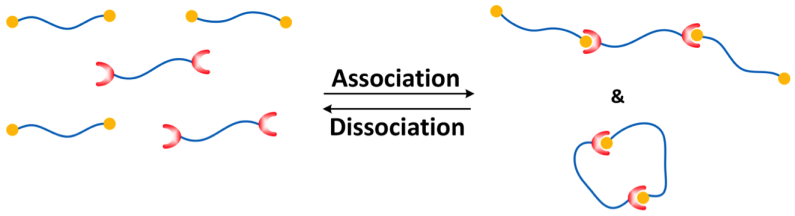

Figure 1.9: Schematic depicting the association and disassociation of end-associative telechelic polymers. Functional groups on the chains may be self-associative or pairwise associative, forming megasupramolecules in solution.

nerable to chain scission) or too short (and thus primarily forming ineffective rings[12,62] or networks[63]). The solvent quality of the backbone in the fluid of choice also affects the rheological behavior and vulnerability to chain scission through changes in the swelling of the coil—too poor of a solvent can cause loss of performance via precipitation.[64] The association strength between polymer units can be manipulated by changing the end-group or by altering the association through interaction with the solvent, which will modify the expected distribution of long linears versus small rings.[12,62] Absence of some end-groups can suppress the formation of long linear chains, but also formation of rings, by acting as end-cappers, usually to the detriment of the total contribution to the rheological properties.[62]

Chapters 2 and 3 discuss considerations in choosing an appropriate backbone length to resist chain scission. Chapter 4 looks at the effects of solvent on the backbone solvent quality and on the effective association strength, in addition to how concentration changes observed association. Chapter 5 outlines the impact of backbone length and end-group fidelity on megasupramolecular formation.

References

[1] E. Villermaux. "Fragmentation". In: *Annual Review of Fluid Mechanics* 39.1 (Jan. 2007), pp. 419–446. ISSN: 0066-4189, 1545-4479. DOI: 10.1146/annurev.fluid.39.050905.110214. URL: http://www.annualreviews.org/doi/10.1146/annurev.fluid.39.050905.110214 (visited on 05/06/2020).

[2] S. Kooij et al. "What Determines the Drop Size in Sprays?" In: *Physical Review X* 8.3 (July 20, 2018). ISSN: 2160-3308. DOI: 10.1103/PhysRevX.8.031019. URL: https://link.aps.org/doi/10.1103/PhysRevX.8.031019 (visited on 06/11/2020).

[3] R. W. Lewis et al. "Polymeric Drift Control Adjuvants for Agricultural Spraying". In: *Macromolecular Chemistry and Physics* 217.20 (Oct. 2016), pp. 2223–2242. ISSN: 10221352. DOI: 10.1002/macp.201600139. URL: https://onlinelibrary.wiley.com/doi/10.1002/macp.201600139 (visited on 03/23/2022).

[4] E. Hilz. "Spray Drift Review: The Extent to Which a Formulation Can Contribute to Spray Drift Reduction". In: *Crop Protection* (2013), p. 9.

[5] V. Bergeron et al. "Controlling Droplet Deposition with Polymer Additives". In: *Nature* 405.6788 (June 2000), pp. 772–775. ISSN: 0028-0836, 1476-4687. DOI: 10.1038/35015525. URL: http://www.nature.com/articles/35015525 (visited on 08/05/2020).

[6] W. Wirth, S. Storpb, and W. Jacobsenb. "Mechanisms Controlling Leaf Retention of Agricultural Spray Solutions". In: *Pesticide Science* 33.4 (1991), pp. 411–420.

[7] M. Xu et al. "Quantifying the Effect of Extensional Rheology on the Retention of Agricultural Sprays". In: *Physics of Fluids* 33.3 (Mar. 1, 2021), p. 032107. ISSN: 1070-6631, 1089-7666. DOI: 10.1063/5.0038391. URL: https://aip.scitation.org/doi/10.1063/5.0038391 (visited on 03/15/2021).

[8] Y. Yeong, J. Burton, and E. Loth. "Drop Impact and Rebound Dynamics on an Inclined Superhydrophobic Surface". In: *Langmuir* 30 (2014), pp. 12027–12038. DOI: 10.1021/la502500z.

[9] M. Sens et al. "Effects of Highly-Heated Fuel and/or High Injection Pressures on the Spray Formation of Gasoline Direct Injection Injectors". In: *Fuel Systems for IC Engines*. Elsevier, 2012, pp. 215–238. ISBN: 978-0-85709-210-6. DOI: 10.1533/9780857096043.6.215. URL: https://linkinghub.elsevier.com/retrieve/pii/B9780857092106500167 (visited on 07/09/2020).

[10] K. K. Chao et al. "Antimisting Action of Polymeric Additives in Jet Fuels". In: *AIChE Journal* 30.1 (Jan. 1984), pp. 111–120. ISSN: 0001-1541, 1547-5905. DOI: 10.1002/aic.690300116. URL: http://doi.wiley.com/10.1002/aic.690300116 (visited on 03/23/2016).

[11] R. S. Marano et al. "Polymer Additives as Mist Suppressants in Metalworking Fluids Part I: Laboratory and Plant Studies - Straight Mineral Oil Fluids". In: *S.A.E. Transactions* 104 (Section 5 1995), pp. 136–146.

[12] M.-H. Wei et al. "Megasupramolecules for Safer, Cleaner Fuel by End Association of Long Telechelic Polymers". In: *Science* 350.6256 (Oct. 2, 2015), pp. 72–75. ISSN: 0036-8075, 1095-9203. DOI: 10.1126/science.aab0642. URL: http://www.sciencemag.org/cgi/doi/10.1126/science.aab0642 (visited on 03/17/2016).

[13] B. Keshavarz et al. "Studying the Effects of Elongational Properties on Atomization of Weakly Viscoelastic Solutions Using Rayleigh Ohnesorge Jetting Extensional Rheometry (ROJER)". In: *Journal of Non-Newtonian Fluid Mechanics* 222 (Aug. 2015), pp. 171–189. ISSN: 03770257. DOI: 10.1016/j.jnnfm.2014.11.004. URL: http://linkinghub.elsevier.com/retrieve/pii/S0377025714002055 (visited on 01/06/2017).

[14] R. P. Mun, J. A. Byars, and D. V. Boger. "The Effects of Polymer Concentration and Molecular Weight on the Breakup of Laminar Capillary Jets". In: (1998), p. 13.

[15] A. N. Rozhkov. "Dynamics and Breakup of Viscoelastic Liquids (A Review)". In: 40.6 (2005), p. 19.

[16] C. Shan et al. "Effects of Droplet Size and Spray Volume Parameters on Droplet Deposition of Wheat Herbicide Application by Using UAV". In: *International Journal of Agricultural and Biological Engineering* 14.1 (2021), pp. 74–81. ISSN: 1934-6344. DOI: 10.25165/j.ijabe.20211401.6129. URL: https://ijabe.org/index.php/ijabe/article/view/6129 (visited on 04/30/2022).

[17] D. Brian et al. "Impact Dynamics and Deposition of Perovskite Droplets on PEDOT:PSS and TiO2 Coated Glass Substrates". In: *Experimental Thermal and Fluid Science* 105 (July 2019), pp. 181–190. ISSN: 08941777. DOI: 10.1016/j.expthermflusci.2019.03.021. URL: https://linkinghub.elsevier.com/retrieve/pii/S0894177718319745 (visited on 04/30/2022).

[18] S. Chandra. "Coating Deposition by Thermal Spray Processes". In: *Annual Review of Heat Transfer* 20.1 (2017), pp. 121–148. ISSN: 1049-0787. DOI: 10.1615/AnnualRevHeatTransfer.2018019747. URL: http://www.dl.begellhouse.com/references/5756967540dd1b03,562e7b3835dec96e,5e195ff86bce1ea9.html (visited on 04/30/2022).

[19] H. Yu, H.-L. Yen, and Y. Li. "Deposition of Bronchiole-Originated Droplets in the Lower Airways during Exhalation". In: *Journal of Aerosol Science* 142 (Apr. 2020), p. 105524. ISSN: 00218502. DOI: 10.1016/j.jaerosci.2020.105524. URL: https://linkinghub.elsevier.com/retrieve/pii/S0021850220300136 (visited on 04/30/2022).

[20] R. Crooks and D. V. Boger. "Influence of Fluid Elasticity on Drops Impacting on Dry Surfaces". In: *Journal of Rheology* 44.4 (July 2000), pp. 973–996. ISSN: 0148-6055, 1520-8516. DOI: 10.1122/1.551123. URL: http://sor.scitation.org/doi/10.1122/1.551123 (visited on 08/05/2020).

[21] M. I. Smith and V. Bertola. "Effect of Polymer Additives on the Wetting of Impacting Droplets". In: *Physical Review Letters* 104.15 (Apr. 15, 2010). ISSN: 0031-9007, 1079-7114. DOI: 10.1103/PhysRevLett.104.154502. URL: https://link.aps.org/doi/10.1103/PhysRevLett.104.154502 (visited on 08/05/2020).

[22] A. Rozhkov, B. Prunet-Foch, and M. Vignes-Adler. "Impact of Drops of Polymer Solutions on Small Targets". In: *Physics of Fluids* 15.7 (July 2003), pp. 2006–2019. ISSN: 1070-6631, 1089-7666. DOI: 10.1063/1.1580480. URL: http://aip.scitation.org/doi/10.1063/1.1580480 (visited on 08/11/2020).

[23] V. Bertola. "An Experimental Study of Bouncing Leidenfrost Drops: Comparison between Newtonian and Viscoelastic Liquids". In: *International Journal of Heat and Mass Transfer* 52.7-8 (Mar. 2009), pp. 1786–1793. ISSN: 00179310. DOI: 10.1016/j.ijheatmasstransfer.2008.09.028. URL: https://linkinghub.elsevier.com/retrieve/pii/S0017931008005875 (visited on 08/06/2020).

[24] V. Bertola. "Effect of Polymer Concentration on the Dynamics of Dilute Polymer Solution Drops Impacting on Heated Surfaces in the Leidenfrost Regime". In: *Experimental Thermal and Fluid Science* 52 (Jan. 2014), pp. 259–269. ISSN: 08941777. DOI: 10.1016/j.expthermflusci.2013.09.019. URL: https://linkinghub.elsevier.com/retrieve/pii/S0894177713002306 (visited on 09/02/2020).

[25] D. Bartolo et al. "Dynamics of Non-Newtonian Droplets". In: *Physical Review Letters* 99.17 (Oct. 26, 2007), p. 174502. ISSN: 0031-9007, 1079-7114. DOI: 10.1103/PhysRevLett.99.174502. URL: https://link.aps.org/doi/10.1103/PhysRevLett.99.174502 (visited on 07/29/2020).

[26] M. D. Graham. "Drag Reduction in Turbulent Flow of Polymer Solutions". In: *Rheology Reviews* 2 (2004), pp. 143–170.

[27] "Some Distinctive Rheological Concepts and Phenomena". In: *Rheology Series*. Ed. by R. Tanner and K. Walters. Vol. 7. Elsevier, 1998, pp. 159–186. ISBN: 978-0-444-82945-0. DOI: 10.1016/S0169-3107(98)80008-7. URL: https://linkinghub.elsevier.com/retrieve/pii/S0169310798800087 (visited on 04/28/2022).

[28] B. A. Toms. "Some Observations on the Flow of Linear Polymer Solutions through Straight Tubes at Large Reynolds Numbers". In: *Proceedings of the International Congress on Rheology* II (1949), pp. 135–141.

[29] B. A. Toms. "On the Early Experiments on Drag Reduction by Polymers". In: *Physics of Fluids* 20.10 (1977), S3. ISSN: 00319171. DOI: 10.1063/1.861757. URL: http://scitation.aip.org/content/aip/journal/pof1/20/10/10.1063/1.861757 (visited on 03/18/2016).

[30] P. S. Virk. "Drag Reduction Fundamentals". In: *AIChE Journal* 21.4 (July 1975), pp. 625–656.

[31] C. M. White, V. S. R. Somandepalli, and M. G. Mungal. "The Turbulence Structure of Drag-Reduced Boundary Layer Flow". In: *Experiments in Fluids* 36.1 (Jan. 1, 2004), pp. 62–69. ISSN: 0723-4864, 1432-1114. DOI: 10.1007/s00348-003-0630-0. URL: http://link.springer.com/10.1007/s00348-003-0630-0 (visited on 04/29/2022).

[32] L. Xi. "Turbulent Drag Reduction by Polymer Additives: Fundamentals and Recent Advances". In: *Physics of Fluids* 31.12 (Dec. 1, 2019), p. 121302. ISSN: 1070-6631, 1089-7666. DOI: 10.1063/1.5129619. URL: http://aip.scitation.org/doi/10.1063/1.5129619 (visited on 07/13/2021).

[33] E. J. Soares. "Review of Mechanical Degradation and De-Aggregation of Drag Reducing Polymers in Turbulent Flows". In: *Journal of Non-Newtonian Fluid Mechanics* 276 (Feb. 2020), p. 104225. ISSN: 03770257. DOI: 10.1016/j.jnnfm.2019.104225. URL: https://linkinghub.elsevier.com/retrieve/pii/S0377025719304197 (visited on 11/19/2020).

[34] P. A. Davidson, ed. *A Voyage through Turbulence*. Cambridge ; New York: Cambridge University Press, 2011. 434 pp. ISBN: 978-0-521-19868-4 978-0-521-14931-0.

[35] J. Southard. "4.8: More on the Structure of Turbulent Boundary Layers-Coherent Structures in Turbulent Shear Flow". In: *Introduction to Fluid Motions, Sediment Transport, and Current-Generated Sedimentary Structures*. LibreTexts, July 19, 2019. URL: https://geo.libretexts.org/Bookshelves/Sedimentology/Book%3A_Introduction_to_Fluid_Motions_and_Sediment_Transport_(Southard)/04%3A_Flow_in_Channels/4.08%3A_More_on_the_Structure_of_Turbulent_Boundary_Layers-_Coherent_Structures_in_Turbulent_Shear_Flow (visited on 05/26/2022).

[36] W. Brostow. "Drag Reduction and Mechanical Degradation in Polymer-Solutions in Flow". In: *Polymer* 24.5 (1983), pp. 631–638. ISSN: 0032-3861. DOI: 10.1016/0032-3861(83)90119-2.

[37] W. Brostow, H. Ertepinar, and R. P. Singh. "Flow of Dilute Polymer Solutions: Chain Conformations and Degradation of Drag Reducers". In: *Macromolecules* 23.24 (1990), pp. 5109–5118. URL: http://pubs.acs.org/doi/abs/10.1021/ma00226a013 (visited on 05/05/2016).

[38] M. W. Liberatore et al. "Turbulent Drag Reduction of Polyacrylamide Solutions: Effect of Degradation on Molecular Weight Distribution". In: (2004), p. 10.

[39] V. N. Kalashnikov. "Degradation Accompanying Turbulent Drag Reduction by Polymer Additives". In: (2002), p. 18.

[40] J. M. J. Den Toonder et al. "Degradation Effects of Dilute Polymer Solutions on Turbulent Drag Reduction in Pipe Flows". In: *Applied scientific research* 55.1 (1995), pp. 63–82. URL: http://link.springer.com/article/10.1007/BF00854224 (visited on 05/05/2016).

[41] T. Moussa and C. Tiu. "Factors Affecting Polymer Degradation in Turbulent Pipe-Flow". In: *Chemical Engineering Science* 49.10 (May 1994), pp. 1681–1692. ISSN: 0009-2509. DOI: 10.1016/0009-2509(93)E0029-C.

[42] S. U. Choi, Y. I. Cho, and K. E. Kasza. "Degradation Effects of Dilute Polymer Solutions on Turbulent Friction and Heat Transfer Behavior". In: *Journal of Non-Newtonian Fluid Mechanics* 41.3 (Feb. 1992), pp. 289–307. ISSN: 03770257. DOI: 10.1016/0377-0257(92)87003-T. URL: https://linkinghub.elsevier.com/retrieve/pii/037702579287003T (visited on 11/19/2020).

[43] S. Jouenne et al. "Degradation (or Lack Thereof) and Drag Reduction of HPAM Solutions During Transport in Turbulent Flow in Pipelines". In: *Oil and Gas Facilities* 4.01 (Feb. 12, 2015), pp. 80–92. ISSN: 2224-4514. DOI: 10.2118/169699-PA. URL: https://onepetro.org/OGF/article/4/01/80/207287/Degradation-or-Lack-Thereof-and-Drag-Reduction-of (visited on 03/24/2022).

[44] T. Q. Nguyen, G. Yu, and H.-H. Kausch. "Birefringence of a Polystyrene Solution in Elongational Flow: Effects of Molecular Weight and Solvent Quality". In: *Macromolecules* 28.14 (July 1995), pp. 4851–4860. ISSN: 0024-9297, 1520-5835. DOI: 10.1021/ma00118a010. URL: http://pubs.acs.org/doi/abs/10.1021/ma00118a010 (visited on 09/13/2016).

[45] T. Q. Nguyen and H.-H. Kausch. "Chain Scission in Transient Extensional Flow Kinetics and Molecular Weight Dependence". In: *Journal of non-newtonian fluid mechanics* 30.2-3 (1988), pp. 125–140. URL: http://www.sciencedirect.com/science/article/pii/0377025788850201 (visited on 09/11/2016).

[46] A. Keller and J. A. Odell. "The Extensibility of Macromolecules in Solution; A New Focus for Macromolecular Science". In: *Colloid & Polymer Science* 263.3 (Mar. 1985), pp. 181–201. ISSN: 0303-402X, 1435-1536. DOI: 10.1007/BF01415506. URL: http://link.springer.com/10.1007/BF01415506 (visited on 04/06/2022).

[47] T. Moussa, C. Tiu, and T. Sridhar. "Effect of Solvent on Polymer Degradation in Turbulent Flow". In: *Journal of Non-Newtonian Fluid Mechanics* 48 (1993), pp. 261–284.

[48] S. A. Vanapalli, M. T. Islam, and M. J. Solomon. "Scission-Induced Bounds on Maximum Polymer Drag Reduction in Turbulent Flow". In: *Physics of Fluids* 17.9 (2005), p. 095108. ISSN: 10706631. DOI: 10.1063/1.2042489. URL: http://scitation.aip.org/content/aip/journal/pof2/17/9/10.1063/1.2042489 (visited on 05/05/2016).

[49] S. A. Vanapalli, S. L. Ceccio, and M. J. Solomon. "Universal Scaling for Polymer Chain Scission in Turbulence". In: *Proceedings of the National Academy of Sciences* 103.45 (Nov. 7, 2006), pp. 16660–16665. ISSN: 0027-8424, 1091-6490. DOI: 10.1073/pnas.0607933103. URL: http://www.pnas.org/cgi/doi/10.1073/pnas.0607933103 (visited on 09/11/2016).

[50] W. Graessley. "Polymer Chain Dimensions and the Dependence of Viscoelastic Properties on Concentration, Molecular Weight and Solvent Power". In: *Polymer* 21.3 (Mar. 1980), pp. 258–262. ISSN: 00323861. DOI: 10.1016/0032-3861(80)90266-9. URL: https://linkinghub.elsevier.com/retrieve/pii/0032386180902669 (visited on 04/28/2021).

[51] M. Bohdanecký, V. Petrus, and B. Sedláček. "Estimation of the Characteristic Ratio of Polyacrylamide in Water and in a Mixed Theta-solvent". In: *Die Makromolekulare Chemie* 184.10 (Oct. 1983), pp. 2061–2073. ISSN: 0025116X, 0025116X. DOI: 10.1002/macp.1983.021841011. URL: http://doi.wiley.com/10.1002/macp.1983.021841011 (visited on 02/04/2021).

[52] C. Clasen et al. "How Dilute Are Dilute Solutions in Extensional Flows?" In: *Journal of Rheology* 50.6 (Nov. 2006), pp. 849–881. ISSN: 0148-6055, 1520-8516. DOI: 10.1122/1.2357595. URL: http://sor.scitation.org/doi/10.1122/1.2357595 (visited on 05/14/2021).

[53] J. Dinic and V. Sharma. "Macromolecular Relaxation, Strain, and Extensibility Determine Elastocapillary Thinning and Extensional Viscosity of Polymer Solutions". In: *Proceedings of the National Academy of Sciences* 116.18 (Apr. 30, 2019), pp. 8766–8774. ISSN: 0027-8424, 1091-6490. DOI: 10.1073/pnas.1820277116. URL: http://www.pnas.org/lookup/doi/10.1073/pnas.1820277116 (visited on 05/05/2021).

[54] J. Dinic and V. Sharma. "Flexibility, Extensibility, and Ratio of Kuhn Length to Packing Length Govern the Pinching Dynamics, Coil-Stretch Transition, and Rheology of Polymer Solutions". In: *Macromolecules* 53.12 (June 23, 2020), pp. 4821–4835. ISSN: 0024-9297, 1520-5835. DOI: 10.1021/acs.macromol.0c00076. URL: https://pubs.acs.org/doi/10.1021/acs.macromol.0c00076 (visited on 05/05/2021).

[55] S. L. Anna and G. H. McKinley. "Elasto-Capillary Thinning and Breakup of Model Elastic Liquids". In: *Journal of Rheology* 45.1 (2001), p. 115. ISSN: 01486055. DOI: 10.1122/1.1332389. URL: http://scitation.aip.org/content/sor/journal/jor2/45/1/10.1122/1.1332389 (visited on 03/22/2016).

[56] G. H. McKinley and T. Sridhar. "Filament-Stretching Rheometry of Complex Fluids". In: *Annual Review of Fluid Mechanics* 34.1 (2002), pp. 375–415. URL: http://www.annualreviews.org/doi/abs/10.1146/annurev.fluid.34.083001.125207 (visited on 03/23/2016).

[57] J. Dinic et al. "Extensional Relaxation Times of Dilute, Aqueous Polymer Solutions". In: *ACS Macro Letters* 4.7 (July 21, 2015), pp. 804–808. ISSN: 2161-1653, 2161-1653. DOI: 10.1021/acsmacrolett.5b00393. URL: http://pubs.acs.org/doi/abs/10.1021/acsmacrolett.5b00393 (visited on 03/17/2016).

[58] J. Dinic, L. N. Jimenez, and V. Sharma. "Pinch-off Dynamics and Dripping-onto-Substrate (DoS) Rheometry of Complex Fluids". In: *Lab on a Chip* 17.3 (2017), pp. 460–473. ISSN: 1473-0197, 1473-0189. DOI: 10.1039/C6LC01155A. URL: http://xlink.rsc.org/?DOI=C6LC01155A (visited on 02/10/2020).

[59] V. Entov and E. Hinch. "Effect of a Spectrum of Relaxation Times on the Capillary Thinning of a Filament of Elastic Liquid". In: *Journal of Non-Newtonian Fluid Mechanics* 72.1 (Sept. 1997), pp. 31–53. ISSN: 03770257. DOI: 10.1016/S0377-0257(97)00022-0. URL: https://linkinghub.elsevier.com/retrieve/pii/S0377025797000220 (visited on 04/02/2021).

[60] R. Learsch. "Investigation in Experimental Conditions and Automation of Dripping-onto-Substrate Rheology". American Chemical Society Spring Meeting (San Diego, CA). Mar. 23, 2022.

[61] J. Dinic, M. Biagioli, and V. Sharma. "Pinch-off Dynamics and Extensional Relaxation Times of Intrinsically Semi-Dilute Polymer Solutions Characterized by Dripping-onto-Substrate Rheometry". In: *Journal of Polymer Science Part B: Polymer Physics* 55.22 (Nov. 15, 2017), pp. 1692–1704. ISSN: 08876266. DOI: 10.1002/polb.24388. URL: http://doi.wiley.com/10.1002/polb.24388 (visited on 03/05/2020).

[62] R. L. A. David. "Associative Polymers as Antimisting Agents and Other Functional Materials via Thiol-Ene Coupling". Pasadena, California: California Institute of Technology, Mar. 7, 2008. 189 pp. URL: http://thesis.library.caltech.edu/2173/.

[63] B. Li. "Ring/Chain versus Network: Architecture Induced by Self- versus Pairwise- Association of Telechelic Polymers". Pasadena, California: California Institute of Technology, 2016. 244 pp.

[64] A. Dupas et al. "Mechanical Degradation Onset of Polyethylene Oxide Used as a Hydrosoluble Model Polymer for Enhanced Oil Recovery". In: *Oil & Gas Science and Technology – Revue d'IFP Energies nouvelles* 67.6 (Nov. 2012), pp. 931–940. ISSN: 1294-4475, 1953-8189. DOI: 10.2516/ogst/2012028. URL: http://ogst.ifpenergiesnouvelles.fr/10.2516/ogst/2012028 (visited on 01/15/2019).